HHS Public Access

Author manuscript

FASEB J. Author manuscript; available in PMC 2023 September 01.

Published in final edited form as:

FASEB J. 2022 September ; 36(9): e22430. doi:10.1096/fj.202200061RR.

Mcm2 hypomorph leads to acute leukemia or hematopoietic stem cell failure, dependent on genetic context

Toshihiro Matsukawa[1,5], **Mianmian Yin**[1,5], **Timour Baslan**[2], **Yang Jo Chung**[1], **Dengchao Cao**[1], **Ryan Bertoli**[1], **Yuelin J. Zhu**[1], **Robert L. Walker**[1], **Amy Freeland**[3], **Erik Knudsen**[3], **Scott W. Lowe**[2,4], **Paul S. Meltzer**[1], **Peter D. Aplan**[1,*]

[1]Genetics Branch, Center for Cancer Research, National Cancer Institute, National Institutes of Health, Bethesda, MD, USA

[2]Cancer Biology and Genetics Program, Sloan-Kettering Institute, NY, USA

[3]Department of Molecular and Cellular Biology, Roswell Park Cancer Institute, Buffalo, NY, USA

[4]Howard Hughes Medical Institute, Chevy Chase, MD, USA

[5]These authors contributed equally to this work.

Abstract

Minichromosome maintenance proteins (Mcm2–7) form a hexameric complex that unwinds DNA ahead of a replicative fork. Deficiency of Mcm proteins leads to replicative stress and consequent genomic instability. Mice with a germline insertion of a Cre cassette into the 3'UTR of the Mcm2 gene (designated *Mcm2*^{Cre}) have decreased Mcm2 expression and invariably develop precursor T-cell lymphoblastic leukemia/lymphoma (pre-T LBL), due to 100–1000 kb deletions involving important tumor suppressor genes. To determine whether mice that were protected from pre-T LBL would develop non-T cell malignancies, we used two approaches. Mice engrafted with *Mcm2*$^{Cre/Cre}$ Lin^{-}Sca-1^{+}Kit^{+} hematopoietic stem/progenitor cells did not develop hematologic malignancy; however, these mice died of hematopoietic stem cell failure by 6 months of age. Placing the *Mcm2*^{Cre} allele onto an athymic *nu*/*nu* background completely prevented pre-T LBL and extended survival of these mice three-fold (median 296.5 vs. 80.5 days). Ultimately, most *Mcm2*$^{Cre/Cre}$;*nu*/*nu* mice developed B cell precursor acute lymphoblastic leukemia (BCP-ALL). We identified recurrent deletions of 100–1000 kb that involved genes known or suspected to be

[*]**Corresponding author**: Peter D. Aplan, Genetics Branch, Center for Cancer Research, National Cancer Institute, National Institutes of Health, Building 37 Room 6002, 37 Convent Drive, Bethesda, MD 20892, USA, PH: 240-760-6889, FAX: 240-541-4477, aplanp@mail.nih.gov.

Author contributions

Peter D. Aplan, Toshihiro Matsukawa, Mianmian Yin conceived and designed the project. Toshihiro Matsukawa, Mianmian Yin, Timour Baslan, Dengchao Cao, Yang Jo Chung., Yuelin J. Zhu., and Robert L. Walker performed experiments, and Toshihiro Matsukawa, Mianmian Yin, Timour Baslan, Ryan Bertoli, Yuelin J. Zhu, Robert L. Walker, and Peter D. Aplan analyzed the data. Amy Freeland and Erik Knudsen established Mcm2 MEFs. Toshihiro Matsukawa wrote the manuscript draft. All authors reviewed, edited and approved the manuscript.

Disclosures

Peter D. Aplan receives royalties from NIH Office of Technology Transfer for the invention of NHD13 mice.

Data and Resource Availability

Mouse strains *NHD13*, *NP23*, *Mcm2*^{Cre} are available from the authors. Nude (*nu*/*nu*) and Scid mice are available from Jackson Labs. The WES data that support the findings of this study are available in SRA with the identifier (https://dataview.ncbi.nlm.nih.gov/object/PRJNA799024?reviewer=5ijd6ml6cu7i48e34qfjbe0l8g) (PRJNA799024).

involved in BCP-ALL, including *Pax5*, *Nf1*, *Ikzf3*, and *Bcor*. Moreover, whole-exome sequencing identified recurrent mutations of genes known to be involved in BCP-ALL progression, such as *Jak1*/*Jak3*, *Ptpn11*, and *Kras*. These findings demonstrate that an $Mcm2^{Cre/Cre}$ hypomorph can induce hematopoietic dysfunction via hematopoietic stem cell failure as well as a "deletor" phenotype affecting known or suspected tumor suppressor genes.

Keywords

Mcm2; DNA stress; bone marrow failure; B-cell precursor acute lymphoblastic leukemia; tumor suppressor gene

Introduction

DNA replication is a semi-conservative process in which daughter cell DNA is synthesized from a parental cell DNA template. [1] Eukaryotic DNA replication initiates with duplication of chromosomal DNA via the formation of a DNA replication "bubble" and bidirectional replication forks. [2] Minichromosome maintenance (MCM) proteins 2–7 form a hexameric complex that is loaded onto parental DNA at the origin of DNA replication as a double hexamer in late M and G1 phases. The MCM2–7 complex functions as a DNA helicase that unwinds parental DNA in advance of replicative polymerase and is essential for initiating DNA replication in S phase. [3,4]

We and others have previously reported that a mouse with an IRES-CreERT2 cassette "knocked into" the 3'UTR of the endogenous murine Mcm2 locus ($Mcm2^{IRES-CreERT2}$, hereafter designated $Mcm2^{Cre}$) results in decreased Mcm2 expression, such that $Mcm2^{Cre/Cre}$ mice have 20–30% the amount of Mcm2 protein compared to wild-type (WT) controls. [5–9] Almost all $Mcm2^{Cre/Cre}$ mice developed a lethal precursor T-cell lymphoblastic leukemia/lymphoma (pre-T LBL) within four months of life. Close analysis of these pre-T LBL revealed that the tumors had undergone 50–1000 kb interstitial deletions of genes well known to be important for mouse and human pre-T LBL, including *PTEN*, *NOTCH1*, and *TCF3*. [8,9] The precise mechanism that causes these interestial deletions in $Mcm2^{Cre/Cre}$ pre-T LBL remains unknown, but it is suspected that limiting amounts of Mcm2 protein lead to replication fork collapse and subsequent DNA double strand breaks (DSB) at the site of replication fork collapse. Repair of two contiguous DNA DSB formed after replication fork collapse, via non-homologous end-joining (NHEJ), leads to the interstitial deletion.

We hypothesized that this unique "deletor" phenotype could be a generally useful mechanism for identifying tumor suppressor genes. However, $Mcm2^{Cre/Cre}$ mice that were predisposed to acute myeloid leukemia (AML) through addition of a *NUP98-HOXD13* (*NHD13*) transgene, which has been shown to induce myelodysplastic syndrome (MDS) and AML, [10,11] did not develop AML. Instead, the $Mcm2^{Cre/Cre}$;*NHD13* developed pre-T LBL at the same age as $Mcm2^{Cre/Cre}$ mice. [9,12] We suspected that the highly penetrant pre-T LBL phenotype was lethal to the mice before a less aggressive malignancy could develop, thus obscuring any AML that might develop in $Mcm2^{Cre/Cre}$;*NHD13* mice. As detailed herein, we used several complementary approaches to test the hypothesis that if $Mcm2^{Cre/Cre}$ mice were prevented from developing pre-T LBL, we could uncover alternate forms of

malignancy in *Mcm2*$^{Cre/Cre}$ mice. The techniques we evaluated to prevent pre-T LBL included allogeneic bone marrow transplantation, and crosses with T-cell deficient mouse strains. In addition, we describe attempt to generate AML, through crossing *Mcm2*$^{Cre/Cre}$ mice to a mouse strain that is predisposed to develop AML.

Materials and Methods

Mouse strains and genotyping

Mcm2$^{Cre/Cre}$, *NUP98-PHF23 (NP23)*, and *NHD13* single transgenic mice were generated on a C57BL/6 background as previously reported. [5,8,10,13] *Mcm2*$^{Cre/Cre}$;*NP23* or *Mcm2*$^{Cre/Cre}$;*NHD13* double transgenic mice were generated by crossing the *NP23* or *NHD13* transgenes onto a *Mcm2*$^{Cre/Cre}$ background. The *Foxn1*^{nu} (*nu*/*nu*) athymic nude mutatation arose in a mouse stock that was closed but not inbred, and were subsequently bred for at least 100 generations before purchase from the Jackson Laboratory. *Prkdc*^{scid} (*Scid*/*Scid*) mice on a C57BL/6 background were purchased from the Jackson Laboratory. Genotyping was performed with using the primers listed (Supplementary Table S10). [9,13] The PCR reaction for *Scid* was digested with *AluI* (New England BioLabs Inc.), and WT or mutant fragments were detected using 4% agarose gel (NuSieve 3:1 Agarose; Lonza). [14] All animal experiments were approved by the National Cancer Institute (Bethesda) Intramural Animal Care and Use Committee.

Assessment of murine leukemia

Peripheral blood from the tail vein was periodically collected in EDTA tubes (RAM Scientific) to assess and monitor mouse health. Complete Blood Counts (CBCs) were measured using a HEMAVET Multispecies Hematology Analyzer (CDC Technologies). Mice were euthanized with carbon dioxide for necropsy when they were moribund or demonstrated signs of illness such as lethargy, weight loss, kyphosis, hunched appearance, or labored breathing. Diagnosis of hematologic malignancies was based on published guidelines for mouse leukemia. [15,16]

Flow Cytometry and cell sorting

Flow cytometry analyses were performed as described previously. [13] Single cells were prepared from each tissue, resuspended with Hanks' balanced salt solution (Lonza) with 2% Fetal Bovine Serum (Gibco) (HF2 buffer), and stained with conjugated antibodies for 30 minutes on ice. The anitbodies used included Ly-6G/Ly-6C (Gr-1)-FITC (Clone-RB6–8C5; eBioscience), CD11b (Mac-1)-PE(Clone-M1/70; eBioscience), CD8a-FITC (Clone-53–6.7; BD Biosciences), CD4-PE (Clone-GK1.5; eBioscience), CD117 (c-Kit)-FITC (Clone-2B8; eBioscience), CD117 (c-Kit)-APC/Cyanine7 (Clone-2B8; eBioscience), Ter119-FITC (Clone-TER119; Biolegend), CD71-PE (Clone-R17217; Biolegend), Ly-6A/E (Sca-1)-PE (Clone-D7; eBioscience), CD45R/B220-FITC (Clone-RA3–6B2; BD Biosciences), CD19-PE (Clone-1D3; eBioscience), CD150 (SLAM)-APC (Clone-TC-15–12F12.2; Biolegend), CD135-BV421 (Clone-A2F10.1; BD Biosciences), CD48-FITC (Clone-HM48–1; eBioscience), Ly-6A/E (Sca-1)-PE/Cyanine7 (Clone-D7; eBioscience), DAPI (564907; BD Biosciences), CD16/32-PE (Clone-93; eBioscience), CD34-FITC (Clone-RAM34; BD Biosciences), CD34-BV605 (Clone-RAM34; BD Biosciences), CD127-BUV737

(Clone-SB/199; BD Biosciences), Streptavidin-PerCP/Cyanine5.5 (Cat#8032909; BD Biosciences), Propidium Iodide (Cat# P3566; Invitrogen), CD45.2-PerCP-Cyanine5.5 (Clone-104; SouthernBiotech), CD45.1-FITC (Clone-A20; eBioscience). The stained single cell suspension was washed twice with HF2 buffer and analyzed using FACScan (BD Biosciences), BD LSRFortessa (BD Biosciences), or Cytek Northern Lights (Cytek) instruments.

B220 positive cells were selected using CD45R(B220) Microbeads (Miltenyi Biotec) and MACS LD column (Miltenyi Biotec) using the manufacturer's recommended protocol. Lineage positive cells were depleted by Lineage Cell Depletion Kit (Miltenyi Biotec) and MACS LD column (Miltenyi Biotec) using the manufacturer's recommended protocol. Lineage negative cells treated above were stained with appropriate antibodies, and sorted with BD FACS AriaFusion (BD Biosciences). Flow cytometry data were analyzed with FlowJo software ver 10.7.2 (BD).

IHC and Histology

Mouse tissue specimens were fixed in 10% Neutral Buffered Formalin (Sigma-Aldrich) and embedded in paraffin. Paraffin-fixed formalin-embedded sections were stained with hematoxylin and eosin (H&E), CD45R/B220 (Clone-RA3–6B2; BD Biosciences), CD3 (Clone-CD3–12; Bio-Rad), Ter119(Clone-TER119; BioLegend), and myeloperoxidase (Cat#A0398; Dako). Stained sections were scanned with Aperio AT2 digital slide scanner (Leica Biosystems) and stored in eSlide Image Management System (Leica Biosystems). The images were viewed with Aperio ImageScope software (Leica Biosystems).

Cell Culture and Cell Lines

Pre-T LBL(6605/4, 6645/4, 7298/2, 6781/3, 2883, 2696, 2641, and 2869) cell lines were established from single-cell suspensions and maintained as previously reported. [9,17]

Sparse Whole-Genome Sequencing (WGS)

Copy Number Aberrations (CNA) was determined by sparse WGS, as previously described. [9] Briefly, 1μg of genomic DNA was sonicated followed by end repair and A-tail addition and ligation of TruSeq adaptors. Libraries were pooled and sequenced, targeting 4 million reads per sample. Data analysis was performed as described previously, [18] using higher resolution bin-boundaries, which allowed analysis of CNA at a segment resolution of ~125kb (five consecutive bins for segmentation).

Whole-Exome Sequencing (WES)

Data processing and variant calling procedure followed the Best Practices workflow recommended by the Broad Institute. Briefly, the raw sequencing reads were mapped to mouse genome build 10 (mm10) by the Burrows-Wheeler Aligner [19] followed by local realignment using the GATK suite [20] from the Broad Institute, and duplicated reads were marked by the Picard tools.

The somatic variants were first filtered with the GATK recommended filtering criteria and further filtered by the following criteria: (1) Minimum fraction of altered reads 0.2; (2)

Minimum number of altered reads in a tumor >= 2; (3) Log transformed FISHER p-value >= 1.5; (4) Variant impact annotation from SnpEff effect prediction is 'High' or 'Moderate'; (5) Exclude SNPs reported in dbSNP build 137 or previously identified as germline variants in the NIH C57BL/6 colony.

PCR, *Igh* gene rearrangement and Sanger sequencing

Genomic DNA was extracted from bone marrow (BM), spleen, thymus, and lymph node with DNeasy Blood & Tissue Kit (Qiagen) according to the manufacturer's instruction. PCR was performed with HiFi Taq polymerase mix (Invitrogen) and primers (Invitrogen) as listed in Supplementary Table S10. *Scid* primers were used as a housekeeping gene to assess DNA quality. Clonal *Igh* segments were identified using PCR-based assays[13]. RNA was extracted using TRIzol (Invitrogen) or RNeasy Mini Kit (Qiagen) with the manufacturer's recommended protocols. cDNA was synthesized by reverse transcriptase using 1 μg RNA with SuperScript III First-Strand Synthesis System (Invitrogen) by reverse transcriptase-PCR (RT-PCR). cDNA quality was based on β-actin. Selected mutations identified by WES were PCR amplified, purified, and confirmed by Sanger sequencing. Real-time quantitative PCR (RQ-PCR) was performed using SYBR Green PCR Master Kit (MilliporeSigma), and Taqman primer-probe (Mcm2; Mm00484815_m1, Ptpn1; Hs00942477_m1) sets with ABI Fast Universal PCR Master Mix on the ABI Fast7500 system (Applied Biosystems/ Life Technologies). Samples were normalized to *Gapdh* or endogenous 18S rRNA with Eukaryotic 18S rRNA Endogenous Control (VIC) (Applied Biosystems). National Cancer Institute Sequencing MiniCore facility performed Sanger sequencing using purified DNA.

Immunoblotting

Pellets of mouse embryonic fibroblasts (MEF) were lysed using RIPA Lysis Buffer (ChemCruz), containing phenylmethylsulfonyl fluoride, protease inhibitor, and sodium orthovanadate. The protein concentration was calculated using Micro BCA Protein Assay Kit (Thermo Fisher Scientific), and samples were prepared with Laemmli Sample Buffer (Bio-Rad). Twenty μg of protein were size-fractinated on 10% SDS-PAGE gels and transferred to nitrocellulose membrane (Thermo Fisher Scientific). After blocking membranes using 5% non-fat dry milk (Bio-Rad) in TBS with 0.1% Tween-20, immunoblotting was performed using the following primary and specific horseradish peroxidase (HRP)-conjugated antibodies and the manufacturer's recommended concentration: MCM2 (Clone-EPR4120; Abcam), β-Actin (Clone-AC-15; Sigma), and Anti-rabbit/mouse IgG HRP-linked Antibody (Cat#7074/#7076; Cell Signaling). MCM2 protein was quantified by ImageJ software (US National Institutes of Health) [21] and normalized against β-Actin.

Transplantation and Engraftment assay

6-week-old female recipient mice which expressed the CD45.1 allele were purchased from the Jackson Laboratory. *Mcm2*$^{Cre/Cre}$ donor cells expressed the CD45.2 allele. The BM, LSK, or LK donor cells were derived from freshly dissected femora and tibiae from 5–6-week-old donor mice and transplanted into lethally irradiated (900 cGy) recipient mice. Recipient mice were injected with 0.2 or 1 × 10E06 CD45.1-WT BM competitor cells and the following CD45.2-donor cells: WT LSK 3500 cells, WT BM 1 million cells,

Mcm2$^{Cre/Cre}$ LSK 3500 cells, *Mcm2*$^{Cre/Cre}$ LK 26000 cells, *Mcm2*$^{Cre/Cre}$;*NHD13* BM 1 million cells. Peripheral blood engraftment and complete blood count (CBC) were assessed at 6, 12, 16, and 24 weeks after transplantation.

Colony-Forming Unit (CFU) assay

Thirty thousand primary BM cells per 35-mm Petri dish were plated in duplicate in Methocult GF M3434 medium (Stemcell Technologies), including the following cytokines; 50 ng/ml rm SCF, 10ng/ml rmIL-3, 10ng/ml rh IL-6, 3 units/ml rhEpo. The plates were incubated at 37°C in a 5% CO_2 incubator, and the number of the colonies were counted on day7 (BFU-E).

Statistics

Data are reported as mean values ± standard deviation. Statistical analysis was carried out with GraphPad Prism software ver 8.4.3 (GraphPad Software, LLC) using the Mantel-Cox log-rank test for Kaplan-Meier curve, unpaired Students' t-test, and one way ANOVA. Holm-Sidak correction of the unpaired Students test was used to correct for multiple hypothesis testing where indicated. p values < .05 were considered to be statistically significant.

Results

Transplant of *Mcm2*$^{Cre/Cre}$ hematopoietic stem/progenitor cells (HSPCs) leads to severe anemia without malignant transformation

Given that the *Mcm2*^{Cre} allele is a germline defect that results in decreased Mcm2 protein in mouse embryo fibroblasts (MEFs) [5] as well as thymocytes [9], we were surprised that we detected no malignancies other than pre-T LBL in *Mcm2*$^{Cre/Cre}$ mice. [9] We considered the possibility that the aggressive, highly penetrant pre-T LBL that develops in *Mcm2*$^{Cre/Cre}$ mice kills the mice before an alternate, less aggressive malignancy of different histology has an opportunity to evolve. To test this hypothesis, we transplanted hematopoietic stem and progenitor cells (HSPCs) from *Mcm2*$^{Cre/Cre}$ mice into wild-type (WT) recipient mice, reasoning that the more differentiated *Mcm2*$^{Cre/Cre}$ HSPCs might generate myeloid malignancies, as opposed to the thymic malignancies that are invariably produced in *Mcm2*$^{Cre/Cre}$ mice, and allow discovery of myeloid tumor suppressor genes.

Hematopoietic stem cells are found in a population of bone marrow cells which are negative for cell surface markers that mark commitment to a terminally differentiated cell lineage (Lineage negative), and are positive for the antigens Sca1 and Kit1; this population is abbreviated LSK. The Lineage$^-$, Sca1$^-$, Kit$^+$(LK) population contains progenitor cells that are committed to a specific hematopoietic lineage (such as myeloid or erythroid), and under normal, non-malignant conditions are not self-renewing stem cells. [22] LSK and LK populations were isolated from WT or *Mcm2*$^{Cre/Cre}$ bone marrow (BM) using fluorescence-activated cell sorting (FACS) and transplanted together with WT competitor cells into lethally irradiated 5-month-old WT recipients. (Supplementary Figure S1A) The *Mcm2*$^{Cre/Cre}$ donor cells expressed the CD45.2 allele of CD45, whereas the WT competitor

cells, and the WT recipients expressed the CD45.1 allele; CD45.1 and CD45.2 proteins can be distinguished by allele-specific CD45 antibodies.

Mice transplanted with LK cells from *Mcm2*$^{Cre/Cre}$ BM did not engraft, indicating that this population did not contain long-term self-renewing cells. However, LSK cells from *Mcm2*$^{Cre/Cre}$ BM were transplantable and self-renewing, and resulted in severe anemia, thrombocytopenia, and a trend toward neutropenia at five months post-transplant (Figure 1A). The mice were euthanized due to morbidity (hunched posture, tachypnea, lethargy) that was detected concurrent with the onset of severe anemia. There was no increase in blast percentage nor difference in myeloid, erythroid, T, and B cell proportions in BM from the *Mcm2*$^{Cre/Cre}$ LSK recipients compared to those of WT LSK recipients, suggesting that the peripheral blood cytopenias were not due to invasion of the BM with malignant cells (Supplementary Figure S1B–C). In addition, parenchymal organs such as liver and spleen (SP) showed no loss of normal histology nor invasion of malignant cells (Supplementary Figure S1D), in contrast to leukocytosis and invasion of parenchymal organs by leukemic cells previously seen in *Mcm2*$^{Cre/Cre}$ mice [9]. Further analysis of *Mcm2*$^{Cre/Cre}$ LSK recipients demonstrated equivalent contribution of WT (CD45.1) and *Mcm2*$^{Cre/Cre}$ cells (CD45.2) in the BM (Supplementary Figure S2A), with a similar distribution of myeloid, T, and B cells. However, there was a decreased contribution of erythroid cells (Ter119^{+}CD71^{+} and Ter119^{+}CD71^{-}) from the CD45.2 (*Mcm2*$^{Cre/Cre}$) donor cells (Supplementary Figure S2A–B). Peripheral blood (PB) showed persistent engraftment of T cells derived from *Mcm2*$^{Cre/Cre}$ cells, demonstrating that lack of malignancy was not due to lack of thymocyte engraftment or development (Figure 1B). Taken together, these results indicate that, in contrast to nearly universal leukemic transformation seen in *Mcm2*$^{Cre/Cre}$ transgenic mice, transplantation of *Mcm2*$^{Cre/Cre}$ LSK cells into WT recipients failed to cause leukemia, despite clear evidence of robust engraftment.

Having determined that the proximal cause of anemia in the *Mcm2*$^{Cre/Cre}$ LSK recipients was not due to infiltration with leukemic cells, we assessed other possible causes of the severe anemia seen in *Mcm2*$^{Cre/Cre}$ LSK recipients. The absolute number of BM cells was decreased by over 50% in the *Mcm2*$^{Cre/Cre}$ LSK recipients (Figure 1c). There was a marked decrease in the number of *Mcm2*$^{Cre/Cre}$-derived erythroid cells compared to WT erythroid cells in the BM of *Mcm2*$^{Cre/Cre}$ LSK recipients (Figure 1d). Consistent with the decrease in Ter119^{+}CD71^{+} cells in the *Mcm2*$^{Cre/Cre}$ LSK BM, there was an absolute decrease in LSK cells and megakaryocyte-erythrocyte progenitors (MEP; Lin^{-}Sca1^{+}cKit^{-} CD16/32^{-}CD34^{-}) (Figure 1E, Supplementary Figure S2B) in the BM of *Mcm2*$^{Cre/Cre}$ LSK recipients. A functional CFU assay demonstrated decreased BFU-E colonies in secondary and tertiary plating from *Mcm2*$^{Cre/Cre}$ LSK recipients (Supplementary Figure S2C). In sum, these findings suggest that the severe anemia in the *Mcm2*$^{Cre/Cre}$ LSK recipients was due to decreased HSPCs in the *Mcm2*$^{Cre/Cre}$ LSK recipients, most prominent in the erythroid lineage.

To rule out the possibility that the phenotype seen in *Mcm2*$^{Cre/Cre}$ LSK recipients could be due to the stress of sorting and *ex vivo* manipulation of the LSK cells, we co-transplanted 10^5 or 10^6 unmanipulated whole BM cells isolated from *Mcm2*$^{Cre/Cre}$ (CD45.2) mice and 10^6 whole BM competitor cells (CD45.1) into congenic CD45.1 recipients (n = 5 for each

BM dose level). (Supplementary Figure S3A) As controls, we transplanted 10^6 whole BM cells isolated from WT CD45.2 mice and 10^6 whole BM CD45.1 competitor cells (n = 5). Two recipients of 10^5 *Mcm2*$^{Cre/Cre}$ BM cells died two weeks post-transplant and showed no evidence of organomegaly at necropsy. All of the remaining mice showed evidence of engraftment at 6 weeks post-transplant (Supplementary Table S1). However, the percent engraftment was markedly diminished in the *Mcm2*$^{Cre/Cre}$ recipients (Supplementary Table S1, Supplementary Figure S3B), and further decreased throughout the observation period (with one exception, discussed below). Despite decreased engraftment, the *Mcm2*$^{Cre/Cre}$ recipients maintained normal PB counts for 12 weeks post-transplant. However, at 13–15 weeks post-transplant, five mice (all *Mcm2*$^{Cre/Cre}$ recipients) were unexpectedly found dead without organomegaly, and the experiment was terminated. At 15 weeks post-transplant, none of the three evaluable *Mcm2*$^{Cre/Cre}$ recipients showed robust engraftment of non-malignant CD45.2 donor cells in PB, BM, or SP (Supplementary Figure S3C), although M36 had engraftment of malignant CD45.2$^+$ T-cells. Two *Mcm2*$^{Cre/Cre}$ recipients (M34, M38) showed profound pancytopenia with no evidence for malignancy (Supplementary Table S1), and one *Mcm2*$^{Cre/Cre}$ recipient (M36) developed pre-T LBL (Supplementary Figure S4). Finally, the absolute number of BM cells from *Mcm2*$^{Cre/Cre}$ recipients was decreased compared to WT (Supplementary Figure S3D). These results indicated that *Mcm2*$^{Cre/Cre}$ hematopoietic cells lose self-renewal potential at ~15 weeks post-transplant.

Decreased absolute number of HSPCs in *Mcm2*$^{Cre/Cre}$ mice

To determine if the decrease in BM cellularity seen in the *Mcm2*$^{Cre/Cre}$ HSPC transplant recipients was also present in non-transplanted *Mcm2*$^{Cre/Cre}$ mice, we evaluated HSPCs derived from 5-week-old *Mcm2*$^{Wt/Wt}$, *Mcm2*$^{Cre/Wt}$, and *Mcm2*$^{Cre/Cre}$ mice. The numbers of unfractionated BM, LSK, and LK cells were all reduced in *Mcm2*$^{Cre/Cre}$ mice compared to the other two genotypes (Supplementary Figure S5A–B). However, although the total number of HSPC was reduced in the *Mcm2*$^{Cre/Cre}$ mice, there was no significant decrease in MEP in *Mcm2*$^{Cre/Cre}$ compared to *Mcm2*$^{Wt/Wt}$. These findings suggest that hematopoiesis from *Mcm2*$^{Cre/Cre}$ mice is impaired and may be exaggerated by the stress of reconstitution imposed by bone marrow transplantation.

Transplantation of LSK and LK cells from *Mcm2*$^{Cre/Cre}$;NHD13 mice leads to B cell precursor acute lymphoblastic leukemia

Mice that express a *NHD13* transgene develop MDS, which progresses to AML, or less commonly pre-T LBL or B cell precursor acute lymphoblastic leukemia (BCP-ALL), in about 70% of mice. [10] Since the NHD13 transgene predisposes mice to develop AML, we previously crossed the NHD13 transgene onto an *Mcm2*$^{Cre/Cre}$ background, reasoning that this strategy may uncover tumor suppressor genes important for AML. [9] However all *Mcm2*$^{Cre/Cre}$;*NHD13* mice developed pre-T LBL, and 26% of *Mcm2*$^{Cre/Cre}$;*NHD13* mice developed a concurrent, independent BCP-ALL. [9] Reasoning that committed hematopoietic progenitors would not be able to differentiate to thymocytes, we transplanted LK cells from a *Mcm2*$^{Cre/Cre}$;*NHD13* donor into WT recipients, using uncommitted *Mcm2*$^{Cre/Cre}$;*NHD13* LSK cells as a control. Recipients developed BCP-ALL with leukocytosis, anemia, and thrombocytopenia at 3–6 months of age (Figure 2A, Supplementary Table S2). Flow cytometry (FCM) displayed expansion of abnormal B cells in BM, SP, thymus (TH), and

lymph node (LN), as well as invasion into nonlymphoid tissues (Figure 2A–B). Analysis of *Igh* gene configuration demonstrated monoclonal rearrangements in the leukemic cells (Supplementary Figure S6A–B, Supplementary Table S2); mice MT1180 and MT1183 had identical clonal *Igh* rearrangements, suggesting that these clones had a common ancestor. Although the conclusion is limited by the small number of recipient mice that we were able to analyze, these findings suggest that LSK and LK cells isolated from *Mcm2*$^{Cre/Cre}$;*NHD13* mice did not induce pre-T LBL, but developed BCP-ALL rather than AML.

Mcm2$^{Cre/Cre}$;*Scid*/*Scid* mice failed to prevent pre-T LBL

We next chose an alternate approach to prevent pre-T LBL. We crossed *Mcm2*$^{Cre/Cre}$ onto a homozygous *Prkdc*^{Scid} (hereafter, *Scid*) background, reasoning that *Scid* mice, deficient in both B and T lymphocytes, will not develop B- or T-cell malignancies, and therefore may develop AML. [23] Mice with 2 alleles of *Scid* (*Mcm2*$^{Cre/Cre}$;*Scid*/*Scid*) were generated by crossing *Mcm2*$^{Cre/Wt}$;*Scid*/+. All *Mcm2*$^{Cre/Cre}$;*Scid*/*Scid* mice developed pre-T LBL with a short life span. (Supplementary Figure S7A–C, Supplementary Table S3). These pre-T LBL were characterized by differentiation to the DP stage of thymocyte development. The *Scid* allele is known to be somewhat “leaky”, [23] and we hypothesized that a relatively rare thymocyte that differentiates beyond the DN stage is now susceptible to the highly penetrant, oncogenic influence of the *Mcm2*$^{Cre/Cre}$ genotype. The presence or absence of the *Scid* allele did not affect hemoglobin (Hgb) or platelet (Plt) counts. (Supplementary Figure S7D)

Mcm2$^{Cre/Cre}$ nude (*nu*/*nu*) mice do not develop pre-T LBL, but instead develop BCP-ALL

Mice with 2 copies of the nude allele (*nu*/*nu*) lack mature T-cells due to a mutated *Foxn1* gene, [24] which is required for development of thymic epithelial cells. We reasoned that placing the *Mcm2*$^{Cre/Cre}$ alleles onto a nude background would prevent pre-T LBL, as nude mice have only a rudimentary thymic remnant and lack normal thymic development. Mice with *Mcm2*$^{Cre/Wt}$ and *Mcm2*$^{Wt/Wt}$ genotypes are phenotypically identical and not prone to malignancy or early death [5,9]; similarly, mice with one copy of the nude allele have normal T cells and hair development. [25,26] For simplicity, *Mcm2*$^{Cre/Cre}$;*nu*/+ and *Mcm2*$^{Cre/Cre}$;+/+ were pooled and designated *Mcm2*$^{Cre/Cre}$, and *Mcm2*$^{Cre/Wt}$;*nu*/*nu* and *Mcm2*$^{Wt/Wt}$;*nu*/*nu* were pooled and designated *nu*/*nu*. Finally, *Mcm2*$^{Wt/Wt}$;+/+, *Mcm2*$^{Wt/Wt}$;*nu*/+, *Mcm2*$^{Cre/Wt}$;+/+, and *Mcm2*$^{Cre/Wt}$;*nu*/+ were pooled and designated WT.

Mcm2$^{Cre/Cre}$ mice had a markedly decreased survival due to pre-T LBL, compared to WT mice (median, 80 days vs. not reached, $P < 0.001$) (Figure 3A, Supplementary Figure S8A–B, Supplementary Table S4). In contrast, *Mcm2*$^{Cre/Cre}$;*nu*/*nu* mice did not develop pre-T LBL and had markedly prolonged survival compared to *Mcm2*$^{Cre/Cre}$, demonstrating that the lack of T cell development in these mice prevents pre-T LBL and dramatically prolonged survival (Figure 3A). Despite a median survival of 296.5 days, >3X longer than *Mcm2*$^{Cre/Cre}$ mice, most *Mcm2*$^{Cre/Cre}$;*nu*/*nu* mice eventually developed BCP-ALL characterized by anemia, thrombocytopenia, hepatomegaly, splenomegaly, and lymphadenopathy. Immunohistochemistry (IHC) and FCM demonstrated invasion of B220^{+} blasts in BM, SP, TH, LN, and parenchymal tissues (Figure 3B–C. Supplementary Table S4). Consistent with a diagnosis of BCP-ALL, the mice had clonal *Igh* gene rearrangements (Supplementary Table S5). The immunophenotypes of these BCP-ALL were variable; some

were CD19^{+}B220$^{-/low}$ (e.g., D114 and D118 in Figure 3B), consistent with a pro-B1 ALL; others (e.g., D095, 556, and D567 in Fig 3B) were CD19^{+}B220^{+} or CD19^{-}B220^{+}, more consistent with a pro-B2 ALL.

In addition to the leukemic mice described above, one *Mcm2*$^{Cre/Cre}$;*nu*/*nu* mouse (572) developed a solid ocular mass, with significant expansion of Mac-1^{+}Gr-1^{+} cells (Supplementary Figure S9A) but with no pus nor other evidence for infection. The complete blood count (CBC) was normal (Supplementary Table S4), the BM showed normal proportions of myeloid and erythroid cells, and there was no invasion of Mac-1^{+}Gr-1^{+} in the liver or lung (Supplementary Figure S9B), which suggested a chloroma-like disease. Three mice (D014, D049, and D302) died with profound anemia (Hgb 2.2–7.7 mg/dL) (Supplementary Table S4) and decreased erythropoiesis in the BM, accompanied by erythroid expansion and maturation arrest in the spleen (Supplementary Figure S9C). However, these three cases did not show peripheral leukocytosis, increased blasts in the BM, or infiltration of malignant erythroid cells in non-hematopoietic tissue (Supplementary Figure S9D). Thus, the severe anemia seemed to be due to erythroid maturation arrest as opposed to myeloid leukemia.

Addition of an *NP23* fusion gene accelerates onset of BCP-ALL in *Mcm2*$^{Cre/Cre}$;*nu*/*nu* mice

We attempted to induce myeloid leukemias in *Mcm2*$^{Cre/Cre}$;*nu*/*nu* mice using an (*NUP98-PHF23* or *NP23*) transgene [13] to promote AML. We crossed *Mcm2*$^{Cre/Wt}$;*nu*/+ with *Mcm2*$^{Cre/Wt}$;*nu*/+;*NP23* to generate *Mcm2*$^{Cre/Cre}$;*nu*/*nu*;*NP23* mice. The *NP23* transgene alone leads to early death from leukemia compared to WT mice (median, 248 days and not reached, $P < 0.001$) (Figure 4A). Placing the *NP23* transgene on an *Mcm2*$^{Cre/Cre}$ background had no effect on survival compared to *Mcm2*$^{Cre/Cre}$; most mice developed an aggressive pre-T LBL (Supplementary Table S6). Similar to *Mcm2*$^{Cre/Cre}$;*NHD13* mice, [9] 27% (3/11) of the *Mcm2*$^{Cre/Cre}$;*NP23* mice developed BCP-ALL (Supplementary Figure S10, Supplementary Table S6). Addition of the *NP23* transgene to *Mcm2*$^{Cre/Cre}$;*nu*/*nu* mice largely reversed the survival advantage seen in *Mcm2*$^{Cre/Cre}$;*nu*/*nu* (median, 130.5 days vs 296.5 days, $P < 0.001$), and most *Mcm2*$^{Cre/Cre}$;*nu*/*nu*;*NP23* mice developed BCP-ALL. There was no clear difference between the *Mcm2*$^{Cre/Cre}$;*nu*/*nu* and *Mcm2*$^{Cre/Cre}$;*nu*/*nu*;*NP23* BCP-ALL in terms of CBC, immunophenotype, or *Ig* V region usage (Supplementary Tables S4–7). Of note, similar to the previous characterization of pro-B1 ALL, [27] all the CD19^{+}B220$^{-/low}$ BCP-ALL in this study utilized V segments located at the 3’ end of the V region cluster (Supplementary Figure S11). [28] A summary of leukemic phenotypes is shown in Supplementary Figure S12.

NGS identification of recurrent, acquired mutations.

We used sparse WGS to detect recurrent CNA (Figure 5). The minimal resolution of this technique is approximately 100kb, and we previously found that most mutations identified by sparse WGS in pre-T LBL associated with Mcm2 deficiency were interstitial deletions of 100–1000 kb. [9] We defined common deletions or gains to be those that occurred in at least two samples from mice with the Mcm2 hypomorph (*Mcm2*$^{Cre/Cre}$;*NHD13*, *Mcm2*$^{Cre/Cre}$;*nu*/*nu* or *Mcm2*$^{Cre/Cre}$;*nu*/*nu*;*NP23*). In sum, we identified 24 recurrent CNA, most commonly deletions (Supplementary Table S8). We identified no recurrent

CNA in the erythroid hyperplasia samples. Note that the frequency of recurrent deleted regions is markedly less in mice with the *Mcm2*$^{Cre/Wt}$;*NHD13* genotype (1.25 CNA per tumor; Supplementary Table S8), which would be expected to have WT Mcm2 function. Recurrently deleted regions encompassed numerous genes that are well known to be inactivated in human B cell malignancies, including *Pax5*, *Ikzf3*, *Nf1*, and *Sh2b3.* [29,30] High-resolution views show that important tumor suppressor genes are often the only gene present within a commonly deleted region. (Figure 5B–C) In addition, we have previously shown that *Bcor*, although not frequently mutated in human B cell malignancies, was frequently inactivated via single nucleotide variation (SNV) or small indel in murine pro-B1 ALL [27]; focal *Bcor* deletions were identified in all three *Mcm2*$^{Cre/Cre}$ genotype groups in this study (Supplementary Figure S13A). Similarly, *DNMT3a*, which is commonly mutated in human myeloid malignancies but not in human B cell malignancy, was recurrently deleted. Finally, *Ptpn1*, although not commonly mutated in human B cell malignancies, was recurrently deleted in all 3 *Mcm2*$^{Cre/Cre}$ genotypes (Supplementary Figure S13B). We confirmed that the recurrent *Ptpn1* deletions were associated with decreased *Ptpn1* expression by qRT-PCR (Supplementary Figure S13C).

We used WES to detect small indels and SNVs associated with the development of BCP-ALL in *Mcm2*$^{Cre/Cre}$;*nu*/*nu* and *Mcm2*$^{Cre/Cre}$;*nu*/*nu*;*NP23* mice. We identified recurrent Tier 1 mutations in genes known or suspected to be involved in B-cell malignancy, such as *Ikzf3*, *Pax5*, and *Bcor* (Supplementary Table S9). We identified non-recurrent (i.e., only one example) mutations in genes well known to be involved in B-cell leukemia, including *Kras*, *Tp53bp1*, *Ptpn11*, and *Notch1*. Figure 6 shows an integrated summary of genotype, immunophenotype, WES, and sparse WGS findings with respect to genes known or suspected to be involved in B-cell malignancies and B cell differentiation. Several genes, such as *Sh2b3* or *Nf1,* were shown to be inactivated via either SNV or large interstitial deletion, whereas other genes (*Jak1*, *Kras*, and *Ptpn11*) were only mutated via SNV missense mutation, and others (*Ptpn1*, *Ebf1*, and *Pax5*) only mutated via large interstitial deletion. As noted previously, as opposed to B cell leukemia that developed in mice with an *Mcm2*$^{Cre/Cre}$ genotype which universally showed CNA involving relevant genes, the B cell leukemia that developed in mice with an *Mcm2*$^{Cre/Wt}$ genotype had no evidence of recurrent, focal CNA.

Taken together, these integrated findings demonstrate that most BCP-ALL samples contained mutations in one or more pathways known to be critical determinants for human B cell malignancies, such as impaired B cell differentiation, increased stem cell self-renewal, hyperproliferation, and cytokine-independent growth, and that the most common form of oncogenic mutation in mice with the *Mcm2*$^{Cre/Cre}$ genotype are recurrent interstitial deletions of 100–1000 kb.

MEFs from *Mcm2*$^{Cre/Cre}$ mice do not display a deletor phenotype.

We considered the possibility that the failure to detect nonlymphoid malignancies in *Mcm2*$^{Cre/Cre}$ mice may be due to a less severe “deletor” phenotype in nonlymphoid tissues. To test this possibility, we established MEFs from *Mcm2*$^{Wt/Wt}$, *Mcm2*$^{Cre/Wt}$, and *Mcm2*$^{Cre/Cre}$ mice. Given that we planned to examine MEFs that had been passed *in vitro*,

we first verified that the Mcm2 protein defieicncy present in *Mcm2*$^{Cre/Cre}$ pre-T LBL persisted after passage *in vitro*. Since no pre-T LBL malignancies developed in *Mcm2*$^{Wt/Wt}$ or *Mcm2*$^{Cre/Wt}$ mice, we used pre-T LBL cell lines established from *SCL*/*LMO1* mice [17] as controls. Supplementary Figure S14A shows that the growth rates of the *SCL*/*LMO1* cell lines were similar to the *Mcm2*$^{Cre/Cre}$ cell lines, and that the decreased mRNA and protein in *Mcm2*$^{Cre/Cre}$ cell lines persisted *in vitro* (Supplementary Figure S14B–C).

Similar to the findings with *Mcm2*$^{Cre/Cre}$ pre-T LBL cell lines, *Mcm2*$^{Cre/Cre}$ MEFs showed ~20% as much Mcm2 mRNA and protein as *Mcm2*$^{Wt/Wt}$ MEFs, demonstrating persistence of the Mcm2 protein deficiency *in vitro* (Supplementary Figure S15A–B). We considered the possibility that interstitial deletions might occur in fibroblasts but are not identified in bulk genomic DNA because MEFs are polyclonal (in contrast to the clonal expansion of lymphoid malignancies with recurrent CNA). Therefore, we isolated single-cell clones from *Mcm2*$^{Wt/Wt}$, *Mcm2*$^{Cre/Wt}$, and *Mcm2*$^{Cre/Cre}$ MEFs (Supplementary Figure S15C) and analyzed 5 clones of each genotype by sparse WGS analysis as shown in Supplementary Figure S15D. There are very few CNA in any clones and no difference in the number or region of CNA correlated with MEF genotype. Small CNA may not be visibly apparent at the whole genome survey level shown in Supplementary Figure S15D. Higher resolution at the individual chromosome level was analyzed, and again no recurrent deletions were identified in the MEF samples. Supplementary Figure S15E–F show high-resolution views of genes commonly deleted in BCP-ALL (*Ptpn1*) and pre-T LBL (*Pten*), respectively.

Discussion

We and others have previously shown that mice deficient for Mcm proteins are prone to chromosomal abnormalities and consequent malignancies. [31,32] In particular, mice with an Mcm2 hypomorphic allele [5] develop pre-T LBL early in life due to recurrent interstitial deletions of critical tumor suppressor genes. [8,9] Interestingly, despite the fact that the Mcm2 hypomorph is a germline defect, the only malignancies we could document in *Mcm2*$^{Cre/Cre}$ mice on a C57BL/6 background were pre-T LBL. One factor that has been reported to be relevant for tumor development in other Mcm mutant mouse models is the mouse strain background; for instance, *Mcm4*$^{Chaos3/Chaos3}$ mice develop mammary tumors on a C3H background, but primarily show perinatal lethality and microopthalmia on a C57BL/6 background. [31,33] Interestingly, a different Mcm4 mutation (*Mcm4*^{D573H} as opposed to *Mcm4*$^{Chaos3/Chaos3}$) leads to pre-T LBL on a mixed C57BL/6 x FVB/N or C57BL/6 × 129S1/SvImJ background. [34] An additional possibility for the thymus specificity of the *Mcm2*$^{Cre/Cre}$ malignancies is that a tissue with rapidly dividing cells, such as the thymus, has increased susceptibility to this unique “deletor” phenotype. We hypothesized that if the *Mcm2*$^{Cre/Cre}$ cells were “protected” from pre-T LBL, that they may develop alternate forms of malignancy due to deletion of other, tissue-restricted tumor suppressor genes, such as *Apc* or *Brca1*.

Although *Mcm2*$^{Cre/Cre}$ LK cells did not engraft, *Mcm2*$^{Cre/Cre}$ LSK cells engrafted with normal hematopoietic PB indices until 5 months post-transplant, at which time the mice became clinically ill with anemia, thrombocytopenia, and borderline neutropenia. Analysis of HSPC showed decreased long-term hematopoietic stem cell (LT-HSC) and MEP

populations; similar results were subsequently obtained with transplant of unfractionated *Mcm2*$^{Cre/Cre}$ BM. Analysis of young (we were limited to studying mice younger than 6 weeks of age as pre-T LBL cells begin to infiltrate *Mcm2*$^{Cre/Cre}$ BM by this age) *Mcm2*$^{Cre/Cre}$ BM similarly demonstrated decreased LT-HSC and MEP in the *Mcm2*$^{Cre/Cre}$ mice. We conclude that the Mcm2 hypomorph leads to failure of HSPC at approximately five months of age, which is obscured by the pre-T LBL that generally emerges by three months of age. The decreased number and early failure of LT-HSC and MEP in the *Mcm2*$^{Cre/Cre}$ mice is similar to findings with an Mcm3 hypomorph, which showed neonatal erythroid failure and poor engraftment of Mcm3 deficient HSC, and we speculate that this hematopoietic failure is due to cumulative replicative stress. [35]

Given that homozygous *Scid* mice have a marked decrease in the number of T and B cells, [23] we predicted that placing the *Mcm2*^{Cre} allele on homozygous *Scid* background might protect the mice from developing pre-T LBL, and allow them to live past the 3–4 month lifespan, at which point they may develop other forms of malignancy. However, all *Mcm2*$^{Cre/Cre}$;*Scid*/*Scid* mice developed pre-T LBL with age of onset slightly early than *Mcm2*$^{Cre/Cre}$ mice. Although somewhat surprising, the *Scid* defect is known to be leaky, [23] and prior crosses of thymic oncogenes onto a *Scid* background had resulted in pre-T LBL, albeit at later onset. [14] In addition, *Scid/Scid* mice are known to be sensitive to ionizing radiation due to defective NHEJ caused by the mutant *Prkdc*^{scid} allele[36]; therefore, it is possible that *Mcm2*$^{Cre/Cre}$;*Scid*/*Scid* mice may have a higher mutation burden and earlier onset of pre-T LBL than *Mcm2*$^{Cre/Cre}$ mice.

Nude (*nu*/*nu*) mice lack mature T-cells due to *Foxn1* deficiency, which leads to dysfunction of thymic epithelial cells. [37] All *Mcm2*$^{Cre/Cre}$;*nu*/*nu* mice were protected from developing T cell malignancy, and had a median life span of 296 vs. 80 days. We suspect that the failure of *Mcm2*$^{Cre/Cre}$;*nu*/*nu* mice to develop a T cell malignancy is due to the fact that *nu/nu* mice lack T cells. *In contrast* to *Scid/Scid* mice, *nu/nu* were maintained on an inbred *nu/nu* background. Therefore, it remains possible that the failure to develop T cell malignancy is independent of the *Foxn1* deficiency and is instead due to an uncharacterized strain difference between C57BL/6 and *nu/nu* mice. Despite this more prolonged survival, most *Mcm2*$^{Cre/Cre}$;*nu*/*nu* mice developed BCP-ALL. Three *Mcm2*$^{Cre/Cre}$;*nu*/*nu* mice developed severe anemia without evidence of leukemic transformation; this observation is reminiscent of the severe anemia that developed in the *Mcm2*$^{Cre/Cre}$ LSK transplant experiment; we speculate that similar to the transplant experiment, the longer survival uncovers the HSC and erythroid failure phenotype. Intriguingly, a subset of the BCP-ALL samples had a CD19^{+}B220$^{-/low}$ phenotype, which is consistent with a B1 lymphocyte progenitor. [38] Leukemias of B1-progenitor origin have recently been described and are characterized by skewed utilization of V_H segments during VDJ recombination, with preferential usage of V_H segments at the 3' end of the V_H region [27]. To date, ALL of progenitor B1 origin has only been described in the context of an *NP23* transgene and *Bcor* mutation [27,39]; the current study demonstrates that pro-B1 ALL can occur in other genetic contexts as well.

We used sparse WGS and WES to compare and contrast acquired mutations in the B cell malignancies that arose in different genetic backgrounds (Figure 6). As anticipated based on results obtained with pre-T LBL, [9] interstitial deletions involving important tumor

suppressor genes were common events in *Mcm2*$^{Cre/Cre}$ BCP-ALL, whereas only one gene (*Pax5*) was recurrently deleted in *Mcm2*$^{Cre/Wt}$ mice. These results support the hypothesis that the Mcm2 hypomorph leads to recurrent interstitial deletions. These recurrent deletions involved several known tumor suppressor genes such as *Pax5*, *Bcor*, *Ikzf3*, *Nf1*, *Srcap*, and *Pten*. *Pax5* is one of the most commonly mutated genes in human BCP-ALL, [40] and *IKZF3*, *NF1*, and *PTEN* are also recurrently mutated in human BCP-ALL. [29] *BCOR* (for *BCL6* corepressor) is frequently mutated in human leukemias and lymphoma, including AML, MDS, and pre-T LBL. [41–43] Although *BCOR* is rarely mutated in human B-lineage malignancy, they are detected in human B-cell lymphomas, [44] and acquired inactivating mutations were seen in over 90% of murine pro-B1 ALL. [27] *Srcap* deletions were identified in over 20% of the BCP-ALL samples. Although *SRCAP* deletions are not common in human B cell malignancies, *SRCAP* has recently been identified as a gene implicated in hematopoietic stem cell differentiation that is frequently mutated in human MDS and clonal hematopoiesis. [45,46] Finally, *Ptpn1* was frequently deleted in *Mcm2*$^{Cre/Cre}$ BCP-ALL. Although *PTPN1* mutations are not common in human B cell malignancies, the recurrent and focal nature of these deletions leads us to suspect that *Ptpn1* may be a tumor suppressor gene in BCP-ALL.

In addition to the deletions identified by sparse WGS, we identified additional acquired mutations, primarily SNV and small indels, through WES. Most prominent were monoallelic gain of function mutations involving signaling molecules well known to be involved in human B cell malignancies such as *Jak1*,[47] *Kras*, [29,48] and *Ptpn11.* [48,49] In addition, *Sh2b3* and *Nf1*, two genes known to be recurrently mutated in human BCP-ALL, [29] were found to have both interstitial deletions and SNV, suggesting that these genes may be inactivated by either deletion or point mutations. As shown in Figure 6, most BCP-ALL that occurred in *Mcm2*$^{Cre/Cre}$;*nu*/*nu* mice had at least one mutation in each of three pathways (B-cell differentiation, kinase and signaling, and stem cell differentiation) that have been shown to be important for human BCP-ALL, indicating that the *Mcm2*$^{Cre/Cre}$;*nu*/*nu* mice serve as an excellent model that recapitulates all of the key features of human BCP-ALL. Of note, *Mcm2*$^{Cre/Cre}$;*NHD13* mice can also serve as a reproducible model for human BCP-ALL, [50] with acquired mutations that overlap with those of the *Mcm2*^{CreCre};*nu/nu* mice, but these are generated through a more cumbersome bone marrow transplant model.

Despite the fact that the *Mcm2*$^{Cre/Cre}$ allele is a germline defect, when *Mcm2*$^{Cre/Cre}$ mice were protected from developing pre-T LBL, the only clear malignancy that developed was BCP-ALL. Notably, T and B lymphocytes are both programmed to tolerate the DNA DSB and acquired 100–1000 kb interstitial deletions that occur during normal VDJ recombination which produces mature antigen receptor genes (T cell receptors and immunoglobulins, respectively). [51] We considered the possibility that recurrent interstitial deletions were common in other tissues from *Mcm2*$^{Cre/Cre}$ mice, but were not detectable as there was no malignancy, and no clonal expansion of nonlymphoid cells or tissues, and hypothetical polyclonal interstitial deletions went undetectable. To address this hypothesis, we searched for recurrent interstitial deletions in single-cell clones established from *Mcm2*$^{Cre/Cre}$, *Mcm2*$^{Cre/Wt}$, and *Mcm2*$^{Wt/Wt}$ MEFs, but identified no recurrent interstitial deletions in MEFs from any genotype. T and B lymphocytes are unique in that they are the only mammalian cell types that normally undergo programmed interstital deletions, during the

process of RAG-mediated VDJ recombination which generates mature antigen receptor genes (T cell receptors and immunoglobulins). Although speculative, it is possible that T and B lymphocytes, which are programmed to undergo interstitial deletions, are able to tolerate DNA DSB induced by the Mcm2 hypomorph, whereas non-lymphocytes undergo apoptosis due to DNA DSB induced by the Mcm2 hypomorph.

In sum, we show that protection of *Mcm2*$^{Cre/Cre}$ mice from developing pre-T LBL, through transplantation of committed hematopoietic cells or a modified genetic background, uncovers a previously undocumented failure of hematopoiesis, and reveals a susceptibility to B cell malignancy. The BCP-ALL that develops in *Mcm2*$^{Cre/Cre}$;*nu/nu* mice closely resembles human BCP-ALL in terms of immunophenotype and the spectrum of acquired mutations. We suggest that *Mcm2*$^{Cre/Cre}$ mice might serve as a general model for producing deletions of tumor suppressor genes *in vivo*, if cells can be programmed to tolerate DNA DSB and interstitial deletions, similar to T and B lymphocytes.

Supplementary Material

Refer to Web version on PubMed Central for supplementary material.

Acknowledgments

The authors thank current and former members of the Aplan lab for insightful discussions. We thank the NCI Sequencing Minicore for Sanger sequencing, the NCI Flow cytometry core for cell sorting, the NCI Pathology/Histotechnology Lab (PHL) for IHC, the NCI Transgenic Core for generation of transgenic mice, and Maria Jorge for excellent animal husbandry. This work was supported by the Intramural Research Program of the National Cancer Institute, National Institutes of Health (to Peter D. Aplan, grant numbers ZIA SC0130378, SC010379, and BC 010983), The Naito Foundation (to Toshihiro Matsukawa), and The Uehara Memorial Foundation (to Toshihiro Matsukawa), and the William C. and Joyce C. O'Neil Charitable Trust, Memorial Sloan Kettering Single Cell Sequencing Initiative (to Timour Baslan).

References

1. Macheret M, Halazonetis TD. DNA replication stress as a hallmark of cancer. Annu Rev Pathol. 2015;10:425–48. doi:10.1146/annurev-pathol-012414-040424 [PubMed: 25621662]
2. Bleichert F, Botchan MR, Berger JM. Mechanisms for initiating cellular DNA replication. Science. Feb 24 2017;355(6327)doi:10.1126/science.aah6317
3. Labib K, Tercero JA, Diffley JF. Uninterrupted MCM2–7 function required for DNA replication fork progression. Science. Jun 2 2000;288(5471):1643–7. doi:10.1126/science.288.5471.1643 [PubMed: 10834843]
4. Randell JC, Bowers JL, Rodriguez HK, Bell SP. Sequential ATP hydrolysis by Cdc6 and ORC directs loading of the Mcm2–7 helicase. Mol Cell. Jan 6 2006;21(1):29–39. doi:10.1016/j.molcel.2005.11.023 [PubMed: 16387651]
5. Pruitt SC, Bailey KJ, Freeland A. Reduced Mcm2 expression results in severe stem/progenitor cell deficiency and cancer. Stem Cells. Dec 2007;25(12):3121–32. doi:10.1634/stemcells.2007-0483 [PubMed: 17717065]
6. Ibarra A, Schwob E, Mendez J. Excess MCM proteins protect human cells from replicative stress by licensing backup origins of replication. Proc Natl Acad Sci U S A. Jul 1 2008;105(26):8956–61. doi:10.1073/pnas.0803978105 [PubMed: 18579778]
7. Orr SJ, Gaymes T, Ladon D, et al. Reducing MCM levels in human primary T cells during the G(0)-->G(1) transition causes genomic instability during the first cell cycle. Oncogene. Jul 1 2010;29(26):3803–14. doi:10.1038/onc.2010.138 [PubMed: 20440261]

8. Rusiniak ME, Kunnev D, Freeland A, Cady GK, Pruitt SC. Mcm2 deficiency results in short deletions allowing high resolution identification of genes contributing to lymphoblastic lymphoma. Oncogene. Sep 6 2012;31(36):4034–44. doi:10.1038/onc.2011.566 [PubMed: 22158038]
9. Yin M, Baslan T, Walker RL, et al. A unique mutator phenotype reveals complementary oncogenic lesions leading to acute leukemia. JCI Insight. Dec 5 2019;4(23):e131434. doi:10.1172/jci.insight.131434
10. Lin YW, Slape C, Zhang Z, Aplan PD. NUP98-HOXD13 transgenic mice develop a highly penetrant, severe myelodysplastic syndrome that progresses to acute leukemia. Blood. Jul 1 2005;106(1):287–95. doi:10.1182/blood-2004-12-4794 [PubMed: 15755899]
11. Raza-Egilmez SZ, Jani-Sait SN, Grossi M, Higgins MJ, Shows TB, Aplan PD. NUP98-HOXD13 gene fusion in therapy-related acute myelogenous leukemia. Cancer Res. Oct 1 1998;58(19):4269–73. [PubMed: 9766650]
12. Matsukawa T, Aplan PD. Clinical and molecular consequences of fusion genes in myeloid malignancies. Stem Cells. Nov 2020;38(11):1366–1374. doi:10.1002/stem.3263 [PubMed: 32745287]
13. Gough SM, Lee F, Yang F, et al. NUP98-PHF23 is a chromatin-modifying oncoprotein that causes a wide array of leukemias sensitive to inhibition of PHD histone reader function. Cancer Discov. May 2014;4(5):564–77. doi:10.1158/2159-8290.CD-13-0419 [PubMed: 24535671]
14. Chervinsky DS, Lam DH, Melman MP, Gross KW, Aplan PD. scid Thymocytes with TCRbeta gene rearrangements are targets for the oncogenic effect of SCL and LMO1 transgenes. Cancer Res. Sep 1 2001;61(17):6382–7. [PubMed: 11522630]
15. Morse HC 3rd, Anver MR, Fredrickson TN, et al. Bethesda proposals for classification of lymphoid neoplasms in mice. Blood. Jul 1 2002;100(1):246–58. doi:10.1182/blood.v100.1.246 [PubMed: 12070034]
16. Kogan SC, Ward JM, Anver MR, et al. Bethesda proposals for classification of nonlymphoid hematopoietic neoplasms in mice. Blood. Jul 1 2002;100(1):238–45. doi:10.1182/blood.v100.1.238 [PubMed: 12070033]
17. Chervinsky DS, Lam DH, Zhao XF, Melman MP, Aplan PD. Development and characterization of T cell leukemia cell lines established from SCL/LMO1 double transgenic mice. Leukemia. Jan 2001;15(1):141–7. doi:10.1038/sj.leu.2401997 [PubMed: 11243382]
18. Baslan T, Kendall J, Rodgers L, et al. Genome-wide copy number analysis of single cells. Nat Protoc. May 3 2012;7(6):1024–41. doi:10.1038/nprot.2012.039 [PubMed: 22555242]
19. Li H, Durbin R. Fast and accurate short read alignment with Burrows-Wheeler transform. Bioinformatics. Jul 15 2009;25(14):1754–60. doi:10.1093/bioinformatics/btp324 [PubMed: 19451168]
20. McKenna A, Hanna M, Banks E, et al. The Genome Analysis Toolkit: a MapReduce framework for analyzing next-generation DNA sequencing data. Genome Res. Sep 2010;20(9):1297–303. doi:10.1101/gr.107524.110 [PubMed: 20644199]
21. Schneider CA, Rasband WS, Eliceiri KW. NIH Image to ImageJ: 25 years of image analysis. Nat Methods. Jul 2012;9(7):671–5. doi:10.1038/nmeth.2089 [PubMed: 22930834]
22. Iwasaki H, Akashi K. Hematopoietic developmental pathways: on cellular basis. Oncogene. Oct 15 2007;26(47):6687–96. doi:10.1038/sj.onc.1210754 [PubMed: 17934478]
23. Bosma MJ, Carroll AM. The SCID mouse mutant: definition, characterization, and potential uses. Annu Rev Immunol. 1991;9:323–50. doi:10.1146/annurev.iy.09.040191.001543 [PubMed: 1910681]
24. Kaushik A, Kelsoe G, Jaton JC. The nude mutation results in impaired primary antibody repertoire. Eur J Immunol. Feb 1995;25(2):631–4. doi:10.1002/eji.1830250249 [PubMed: 7875225]
25. Scheiff JM, Cordier AC, Haumont S. The thymus of Nu/+ mice. Anat Embryol (Berl). Jun 2 1978;153(2):115–22. doi:10.1007/BF00343368 [PubMed: 677466]
26. Eaton GJ. Hair growth cycles and wave patterns in “nude” mice. Transplantation. Sep 1976;22(3):217–22. doi:10.1097/00007890-197609000-00001 [PubMed: 788248]
27. Gough SM, Goldberg L, Pineda M, et al. Progenitor B-1 B-cell acute lymphoblastic leukemia is associated with collaborative mutations in 3 critical pathways. Blood advances. Sep 12 2017;1(20):1749–1759. doi:10.1182/bloodadvances.2017009837 [PubMed: 29296821]

28. Johnston CM, Wood AL, Bolland DJ, Corcoran AE. Complete sequence assembly and characterization of the C57BL/6 mouse Ig heavy chain V region. J Immunol. Apr 1 2006;176(7):4221–34. doi:10.4049/jimmunol.176.7.4221 [PubMed: 16547259]
29. Mullighan CG, Goorha S, Radtke I, et al. Genome-wide analysis of genetic alterations in acute lymphoblastic leukaemia. Nature. Apr 12 2007;446(7137):758–64. doi:10.1038/nature05690 [PubMed: 17344859]
30. Zhang J, Mullighan CG, Harvey RC, et al. Key pathways are frequently mutated in high-risk childhood acute lymphoblastic leukemia: a report from the Children's Oncology Group. Blood. Sep 15 2011;118(11):3080–7. doi:10.1182/blood-2011-03-341412 [PubMed: 21680795]
31. Shima N, Alcaraz A, Liachko I, et al. A viable allele of Mcm4 causes chromosome instability and mammary adenocarcinomas in mice. Nat Genet. Jan 2007;39(1):93–8. doi:10.1038/ng1936 [PubMed: 17143284]
32. Chuang CH, Wallace MD, Abratte C, Southard T, Schimenti JC. Incremental genetic perturbations to MCM2–7 expression and subcellular distribution reveal exquisite sensitivity of mice to DNA replication stress. PLoS Genet. Sep 9 2010;6(9):e1001110. doi:10.1371/journal.pgen.1001110
33. Kawabata T, Yamaguchi S, Buske T, et al. A reduction of licensed origins reveals strain-specific replication dynamics in mice. Mamm Genome. Oct 2011;22(9–10):506–17. doi:10.1007/s00335-011-9333-7 [PubMed: 21611832]
34. Bagley BN, Keane TM, Maklakova VI, et al. A dominantly acting murine allele of Mcm4 causes chromosomal abnormalities and promotes tumorigenesis. PLoS Genet. 2012;8(11):e1003034. doi:10.1371/journal.pgen.1003034
35. Alvarez S, Diaz M, Flach J, et al. Replication stress caused by low MCM expression limits fetal erythropoiesis and hematopoietic stem cell functionality. Nat Commun. Oct 12 2015;6:8548. doi:10.1038/ncomms9548 [PubMed: 26456157]
36. Bosma GC, Custer RP, Bosma MJ. A severe combined immunodeficiency mutation in the mouse. Nature. Feb 10 1983;301(5900):527–30. doi:10.1038/301527a0 [PubMed: 6823332]
37. Szadvari I, Krizanova O, Babula P. Athymic nude mice as an experimental model for cancer treatment. Physiol Res. Dec 21 2016;65(Suppl 4):S441–S453. doi:10.33549/physiolres.933526 [PubMed: 28006926]
38. Montecino-Rodriguez E, Fice M, Casero D, Berent-Maoz B, Barber CL, Dorshkind K. Distinct Genetic Networks Orchestrate the Emergence of Specific Waves of Fetal and Adult B-1 and B-2 Development. Immunity. Sep 20 2016;45(3):527–539. doi:10.1016/j.immuni.2016.07.012 [PubMed: 27566938]
39. Yin M, Chung YJ, Lindsley RC, et al. Engineered Bcor mutations lead to acute leukemia of progenitor B-1 lymphocyte origin in a sensitized background. Blood. Jun 13 2019;133(24):2610–2614. doi:10.1182/blood.2018864173 [PubMed: 30992267]
40. Gu Z, Churchman ML, Roberts KG, et al. PAX5-driven subtypes of B-progenitor acute lymphoblastic leukemia. Nat Genet. Feb 2019;51(2):296–307. doi:10.1038/s41588-018-0315-5 [PubMed: 30643249]
41. Grossmann V, Tiacci E, Holmes AB, et al. Whole-exome sequencing identifies somatic mutations of BCOR in acute myeloid leukemia with normal karyotype. Blood. Dec 1 2011;118(23):6153–63. doi:10.1182/blood-2011-07-365320 [PubMed: 22012066]
42. Damm F, Chesnais V, Nagata Y, et al. BCOR and BCORL1 mutations in myelodysplastic syndromes and related disorders. Blood. Oct 31 2013;122(18):3169–77. doi:10.1182/blood-2012-11-469619 [PubMed: 24047651]
43. Kiel MJ, Velusamy T, Rolland D, et al. Integrated genomic sequencing reveals mutational landscape of T-cell prolymphocytic leukemia. Blood. Aug 28 2014;124(9):1460–72. doi:10.1182/blood-2014-03-559542 [PubMed: 24825865]
44. Jallades L, Baseggio L, Sujobert P, et al. Exome sequencing identifies recurrent BCOR alterations and the absence of KLF2, TNFAIP3 and MYD88 mutations in splenic diffuse red pulp small B-cell lymphoma. Haematologica. Oct 2017;102(10):1758–1766. doi:10.3324/haematol.2016.160192 [PubMed: 28751561]

45. Wong TN, Miller CA, Jotte MRM, et al. Cellular stressors contribute to the expansion of hematopoietic clones of varying leukemic potential. Nat Commun. Jan 31 2018;9(1):455. doi:10.1038/s41467-018-02858-0 [PubMed: 29386642]

46. Beauchamp EM, Leventhal M, Bernard E, et al. ZBTB33 is mutated in clonal hematopoiesis and myelodysplastic syndromes and impacts RNA splicing. Blood Cancer Discov. Sep 2021;2(5):500–517. doi:10.1158/2643-3230.BCD-20-0224 [PubMed: 34568833]

47. Xiang Z, Zhao Y, Mitaksov V, et al. Identification of somatic JAK1 mutations in patients with acute myeloid leukemia. Blood. May 1 2008;111(9):4809–12. doi:10.1182/blood-2007-05-090308 [PubMed: 18160671]

48. Paulsson K, Horvat A, Strombeck B, et al. Mutations of FLT3, NRAS, KRAS, and PTPN11 are frequent and possibly mutually exclusive in high hyperdiploid childhood acute lymphoblastic leukemia. Genes Chromosomes Cancer. Jan 2008;47(1):26–33. doi:10.1002/gcc.20502 [PubMed: 17910045]

49. Tartaglia M, Niemeyer CM, Fragale A, et al. Somatic mutations in PTPN11 in juvenile myelomonocytic leukemia, myelodysplastic syndromes and acute myeloid leukemia. Nat Genet. Jun 2003;34(2):148–50. doi:10.1038/ng1156 [PubMed: 12717436]

50. Hunger SP, Mullighan CG. Acute Lymphoblastic Leukemia in Children. N Engl J Med. Oct 15 2015;373(16):1541–52. doi:10.1056/NEJMra1400972 [PubMed: 26465987]

51. Boehm T, Bleul CC. The evolutionary history of lymphoid organs. Nat Immunol. Feb 2007;8(2):131–5. doi:10.1038/ni1435 [PubMed: 17242686]

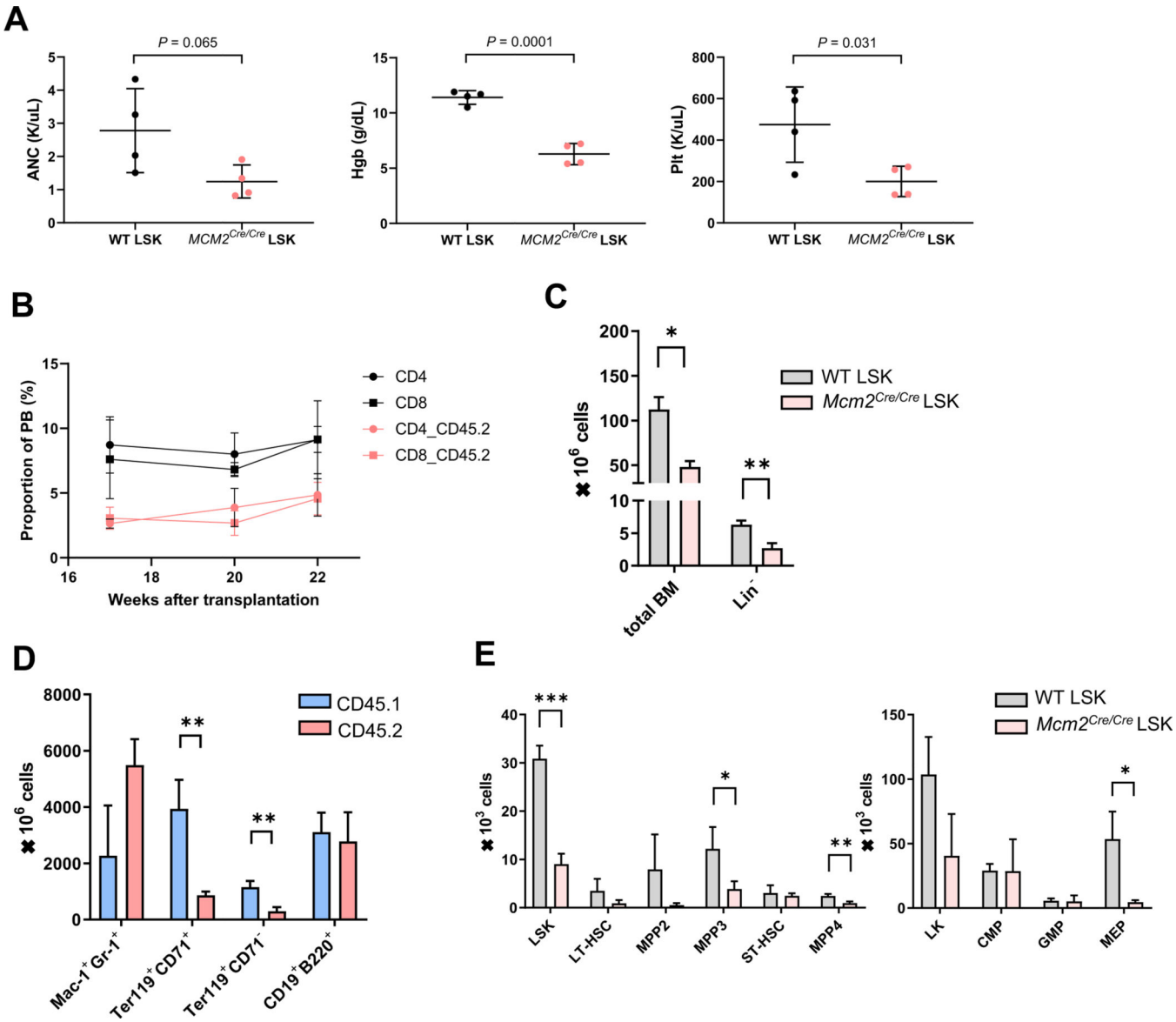

Figure 1. *Mcm2*$^{Cre/Cre}$ LSK cells induce anemia and thrombocytopenia without malignant transformation.

A, Complete blood counts in recipients of WT or *Mcm2*$^{Cre/Cre}$ LSK cells. ANC; absolute neutrophil count, Hgb; hemoglobin, Plt; platelet. **B**, The proportion of total CD4 and CD8 (black lines) and *Mcm2*$^{Cre/Cre}$ derived (CD45.2 positive) CD4 and CD8 cells (red lines) in peripheral blood. **C**, Number of total and Lin$^-$ cells in BM of transplant recipients (n = 3 each). * $P < .05$, ** $P < .01$. **D**, The absolute numbers of myeloid (Mac-1$^+$Gr-1$^+$), erythroid (Ter119$^+$CD71$^+$, Ter119$^+$CD71$^-$), and B lymphoid (CD19$^+$B220$^+$) cells derived from CD45.2 (*Mcm2*$^{Cre/Cre}$) and CD45.1 (competitor) cells. ** $P < .01$. **E**, HSPC subsets in bone marrow (BM) from WT and *Mcm2*$^{Cre/Cre}$ LSK recipients (n = 3 each). ST-/LT-HSC; short/long term-hematopoietic stem cell, MPP; multipotent progenitor, CMP; common myeloid progenitor, GMP; granulocyte/monocyte progenitor, MEP; megakaryocyte/erythroid progenitor

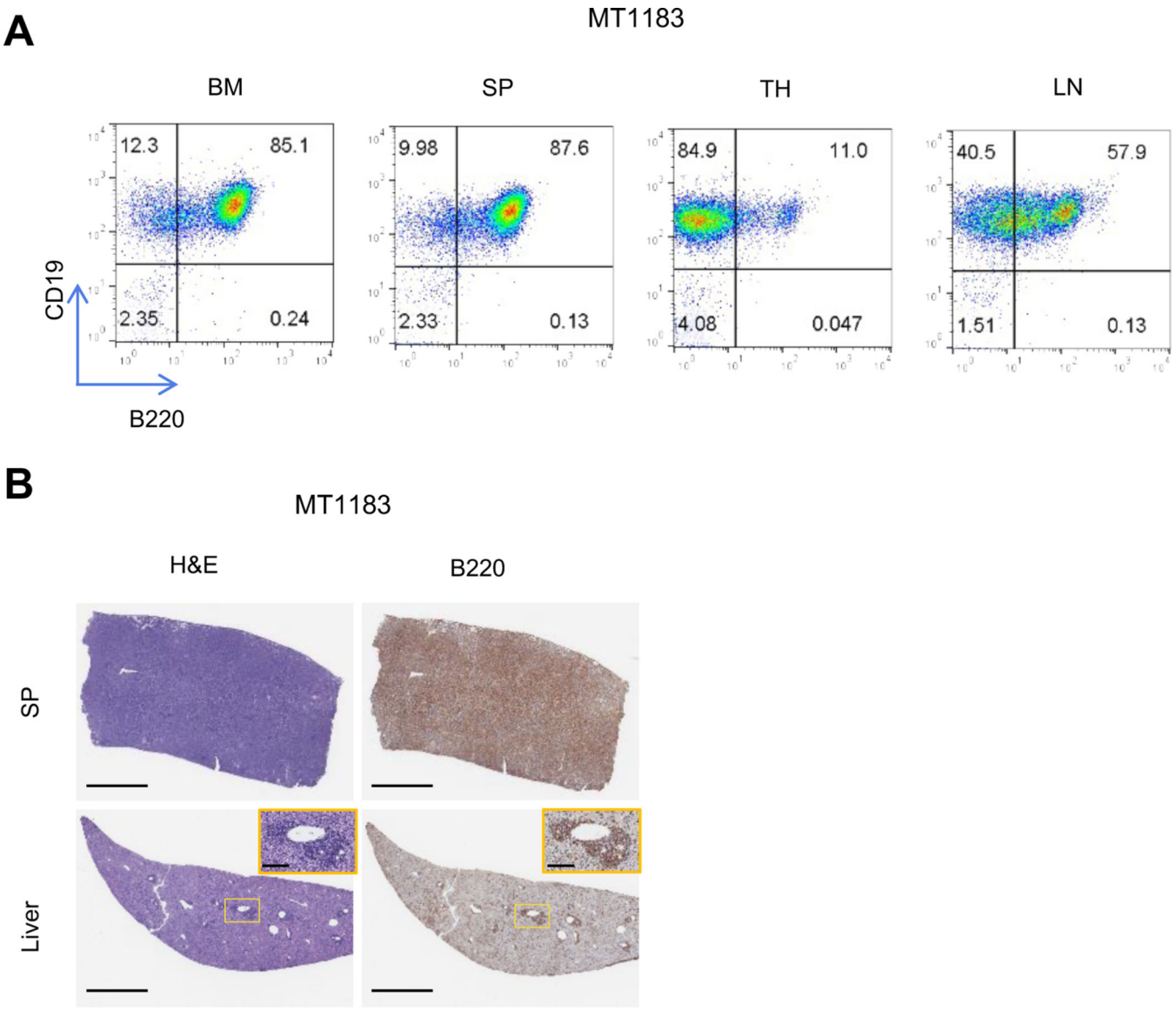

Figure 2. Transplant of *Mcm2*$^{Cre/Cre}$;*NHD13* HSPCs leads to BCP-ALL in recipients.

A, Immunophenotype of BM, SP, TH, and lymph node (LN) from a mouse (MT1183) with BCP-ALL.

B, Hematoxylin and eosin (H&E), and B220 staining of SP and liver from mouse (MT1183) with BCP-ALL. Scale bar 1 mm; inset 300 μm.

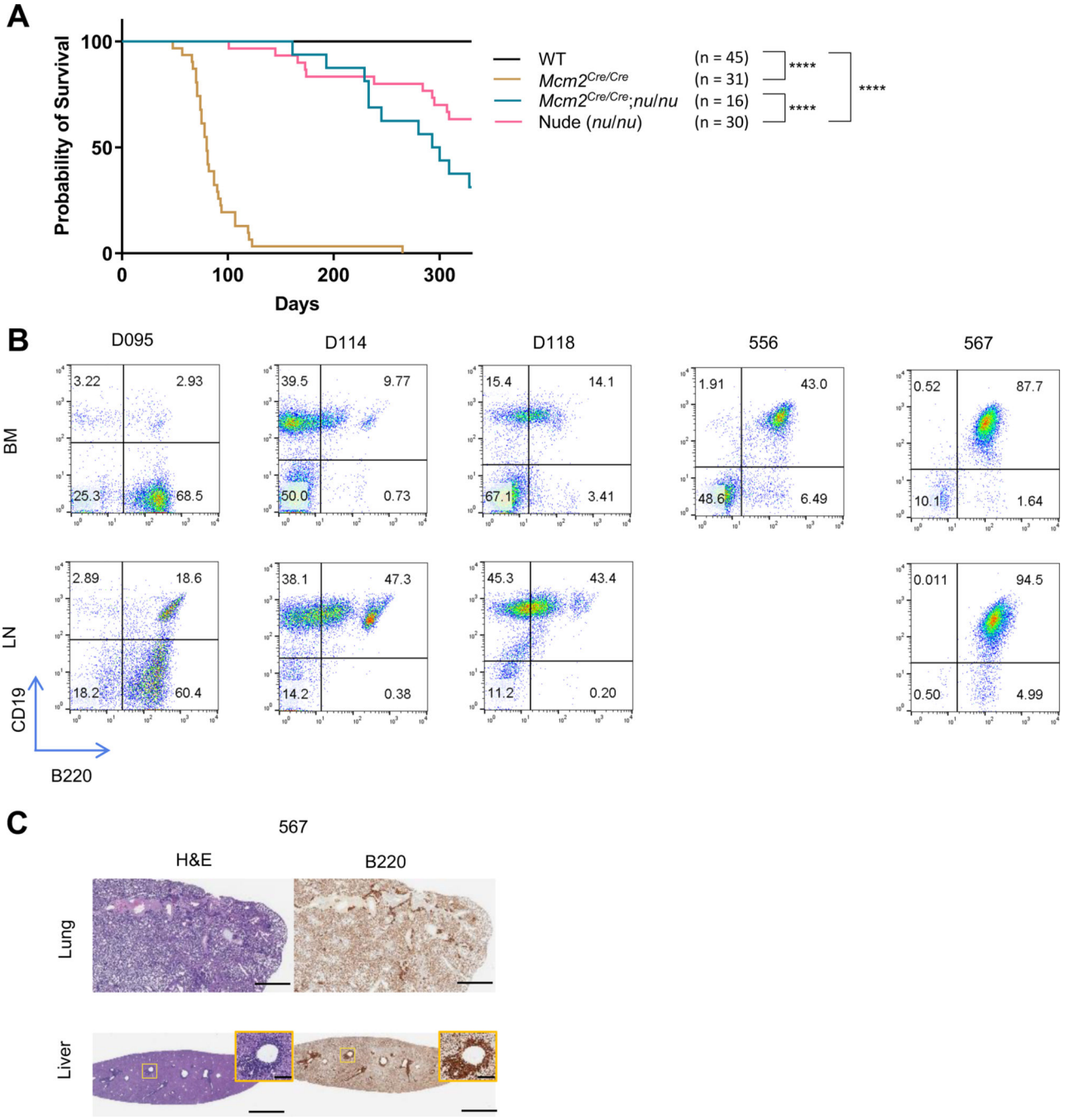

Figure 3. *Mcm2*$^{Cre/Cre}$;*nu/nu* mice have prolonged survival but develop BCP-ALL.

A, Survival of WT, nude (*nu/nu*), *Mcm2*$^{Cre/Cre}$, and *Mcm2*$^{Cre/Cre}$;*nu/nu* mice. Median survival for mice was 296.5 days for *Mcm2*$^{Cre/Cre}$;*nu/nu* and 80.0 days for *Mcm2*$^{Cre/Cre}$. WT and Nude (*nu/nu*) mice did not reach median survival during the observation period. **** $P < .0001$. B, FCM profiles of *Mcm2*$^{Cre/Cre}$;*nu/nu* B-ALL (D95, D114, D118, 556, and 567) demonstrate variable expression of CD19 and B220. (e.g. CD19^{+}B220^{+}, CD19^{-}B220^{+}, CD19^{+}B220^{-}, or CD19^{+}B220$^{-/low}$). **C**, H&E and B220 staining of *Mcm2*$^{Cre/Cre}$;*nu/nu* (567) BCP-ALL. Scale bar, 500 μm; inset 200 μm.

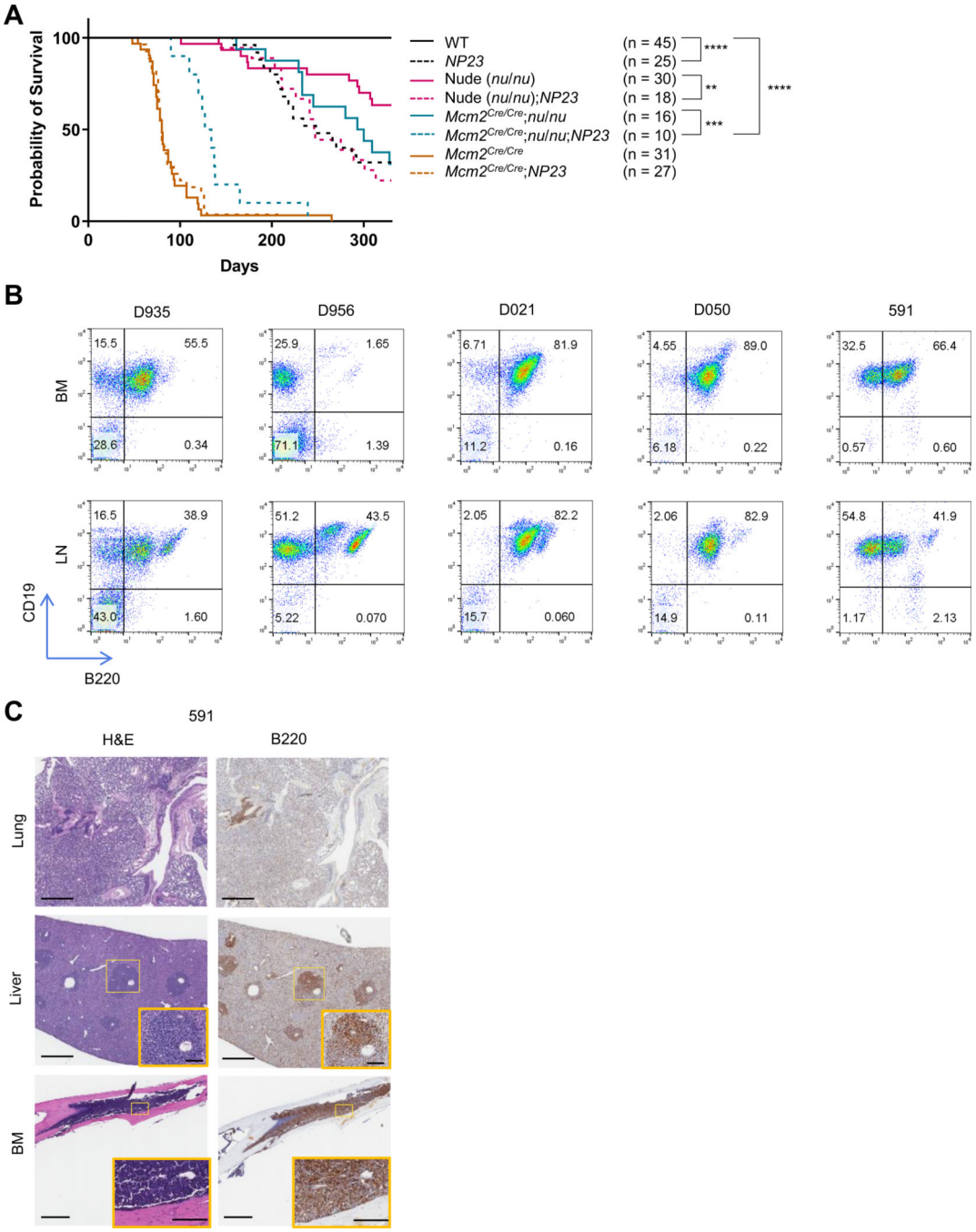

Figure 4. *Mcm2*$^{Cre/Cre}$*;nu/nu;NP23* mice develop BCP-ALL.

A, Survival of *Mcm2*$^{Cre/Cre}$*;nu/nu;NP23* and control genotypes. ** $P < .01$, *** $P < .001$, **** $P < .0001$. **B**, Immunophenotype of *Mcm2*$^{Cre/Cre}$*;nu/nu;NP23* BCP-ALL (D935, D956, D021, D050, and 591), demonstrate a range of CD19 and B220 expression (compare Figure 3B). C, H&E and B220 staining of *Mcm2*$^{Cre/Cre}$*;nu/nu;NP23* B-ALL (591) demonstrates invasion of lung, liver, and BM with B220+ cells. Scale bar, 1 mm; inset 200 μm.

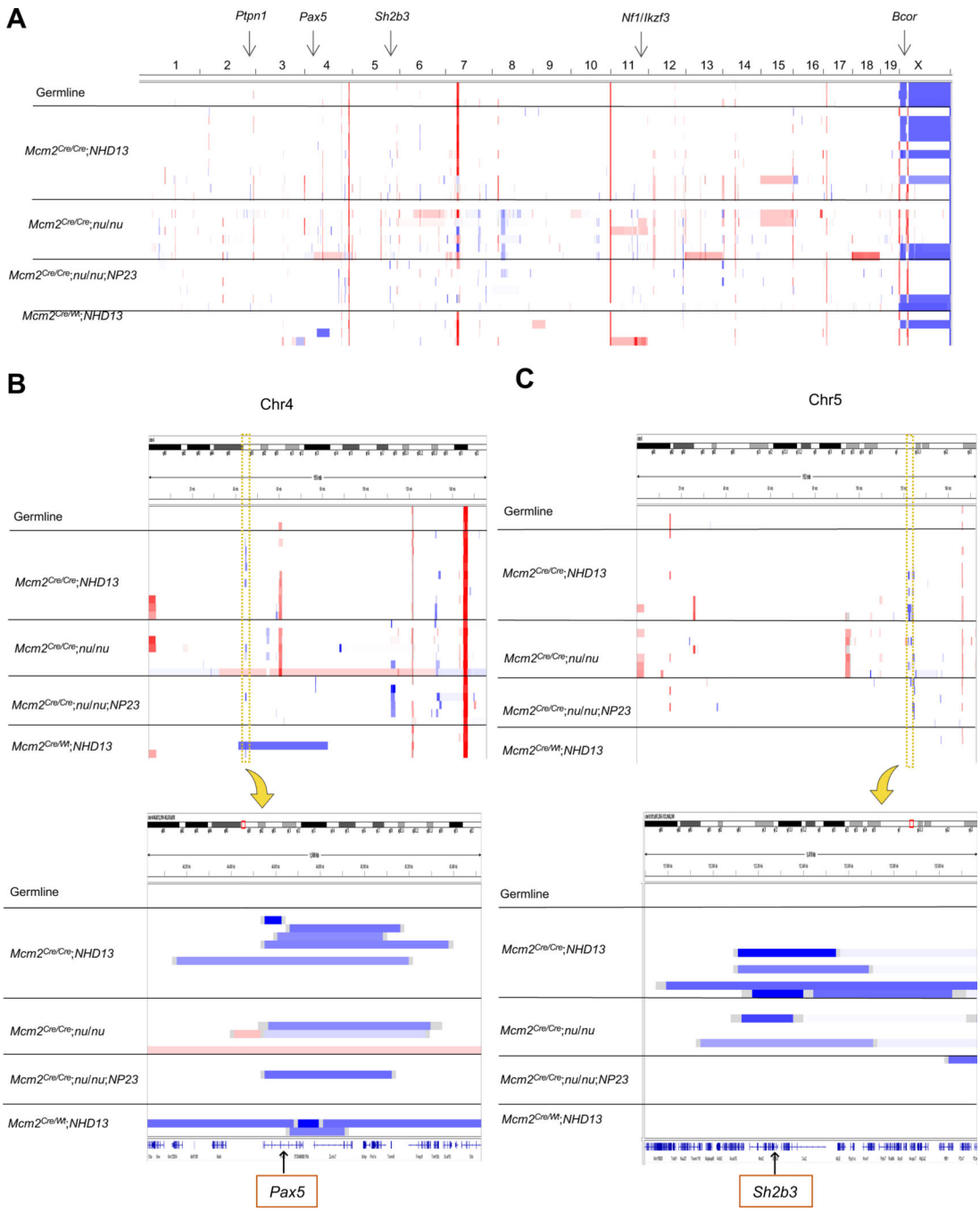

Figure 5. Sparse WGS analysis of B cell leukemias.

A, Whole-genome view of CNA; gains are shown in red, and losses are shown in blue. Boundaries of CNA are highlighted in grey. The color intensity is (log2) proportional to the degree of gain or loss. **B**, Whole chromosome (upper) and high resolution (lower) view of recurrent *Pax5* losses. C, Whole chromosome (upper) and high resolution (lower) view of recurrent *Sh2b3* losses.

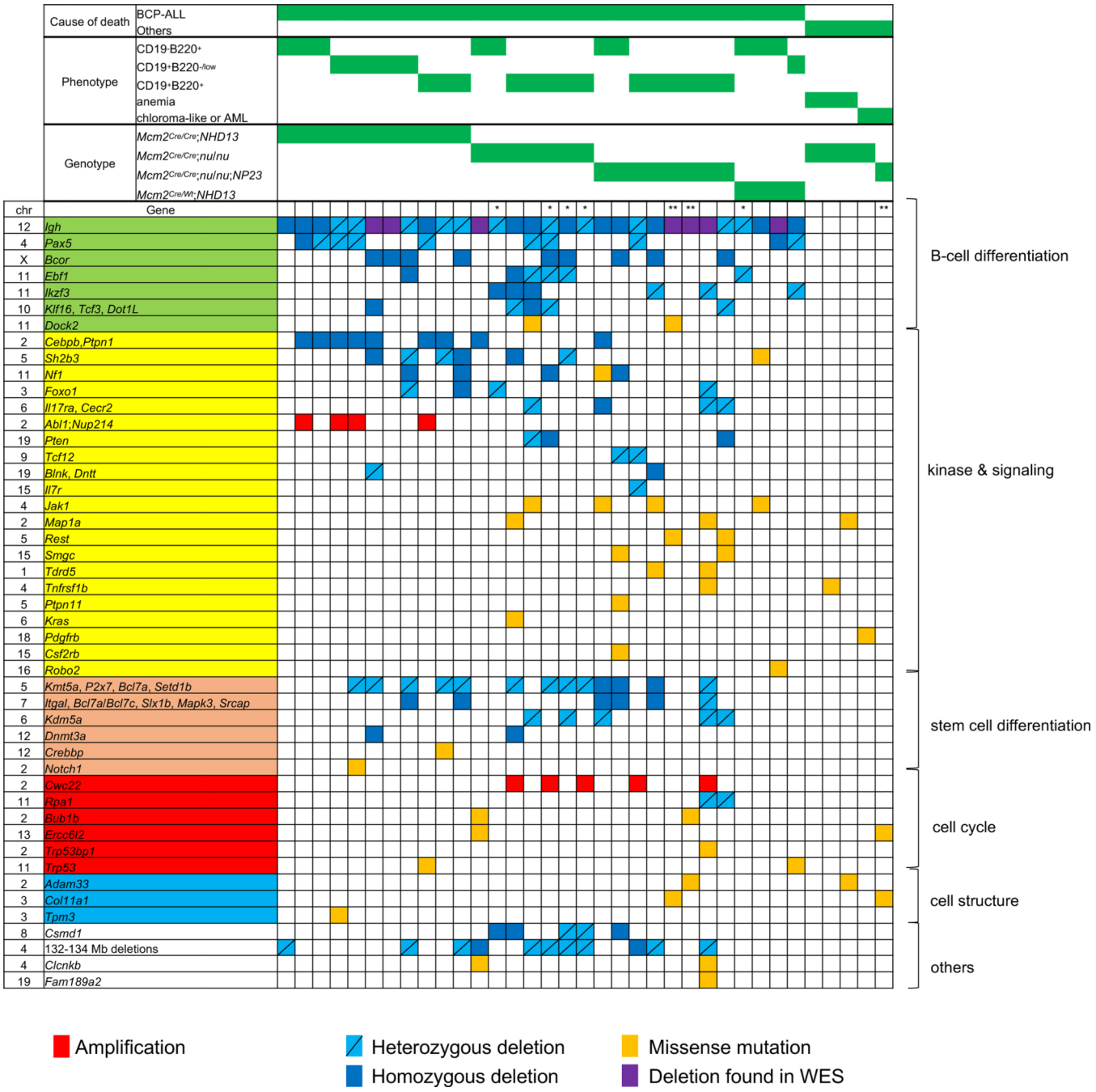

Figure 6. Summary of sparse WGS and WES.

* and ** indicate samples that were assessed by only sparse WGS or WES, respectively. Gene name: green; B-cell differentiation, yellow; kinase and signaling, red; cell cycle, orange; stem cell differentiation, blue; cell structure